2510 *Biochemistry* **2010,** *49,* 2510–2519
DOI: 10.1021/bi902096r

BIOCHEMISTRY
including biophysical chemistry & molecular biology
*Article*

# Molecular Basis of Activation of Endopeptidase Activity of Botulinum Neurotoxin Type E[†]

Roshan V. Kukreja,[‡] Shashi K. Sharma,[§] and Bal Ram Singh*,[‡]

[‡]*Botulinum Research Center and Department of Chemistry and Biochemistry, University of Massachusetts Dartmouth, 285 Old Westport Road, North Dartmouth, Massachusetts 02747, and* [§]*FDA, Center for Food Safety and Applied Nutrition, 5100 Paint Branch Parkway, HFS-712, College Park, Maryland 20740*

*Received August 14, 2009; Revised Manuscript Received February 9, 2010*

ABSTRACT: Botulinum neurotoxins (BoNTs) are a group of large proteins that are responsible for the clinical syndrome of botulism. The seven immunologically distinct serotypes of BoNTs (A−G), each produced by various strains of *Clostridium botulinum*, act on the neuromuscular junction by blocking the release of the neurotransmitter acetylcholine, thereby resulting in flaccid muscle paralysis. BoNTs are synthesized as single inactive polypeptide chains that are cleaved by endogenous or exogenous proteases to generate the active dichain form of the toxin. Nicking of the single chain BoNT/E to the dichain form is associated with 100-fold increase in toxicity. Here we investigated the activation mechanism of botulinum neurotoxin type E upon nicking and subsequent reduction of disulfide bond. It was observed that nicking of BoNT/E significantly enhances its endopeptidase activity and that at the physiological temperature of 37 °C the reduced form of nicked BoNT/E adopts a dynamically flexible conformation resulting from the exposure of hydrophobic segments and facilitating optimal cleavage of its substrate SNAP-25. Such reduction-induced increase in the flexibility of the polypeptide folding provides a rationale for the mechanism of BoNT/E endopeptidase against its intracellular substrate, SNAP-25, and complements current understanding of the mechanistics of interaction between the substrate and BoNT endopeptidase.

Botulinum neurotoxins (BoNTs)[1] are a group of large proteins that are responsible for the clinical syndrome of botulism. Seven antigenically different types (A−G) of BoNTs are produced by various toxigenic strains of *Clostridium botulinum* (*1*). BoNTs are the most potent toxins known to mankind, which act by blocking the release of acetylcholine from the presynaptic terminal of the neuromuscular junction, resulting in flaccid muscle paralysis. In light of the current world security situation, there is a heightened fear of botulinum toxin being used as a biological weapon (*2*), and hence there is an urgent need to develop antidotes to botulism (*3*). Interestingly, however, the therapeutic utility of BoNTs is on the rise as they are being successfully used to treat a variety of neuromuscular disorders and even used as a cosmetic agent to reduce facial wrinkles (*4*−*6*).

Botulinum neurotoxins are synthesized as inactive single polypeptide chains of 150 kDa which are cleaved by proteases to generate the active dichain form of the toxin. Some clostridial strains contain endogenous proteases that nick the neurotoxin (e.g., type A), whereas botulinum neurotoxin type E (BoNT/E) is released from the bacterium in a single chain form that is completely unnicked and must be exposed to exogenous proteases such as trypsin to be activated (*7*, *8*). In the resultant dichain potent neurotoxin, noncovalent interactions (including hydrophobic and ionic interactions and the disulfide bond) link the N-terminal light chain ($M_r$ = 50000) domain to the larger C-terminal heavy chain ($M_r$ = 100000) (*9*).

The mode of action involves binding, internalization, and translocation of BoNTs into nerve cells that is mediated by the heavy chain followed by the metalloprotease activity of the light chain in cytosol to selectively target proteins essential for neuroexocytosis (*1*, *10*). BoNT serotypes A and E act specifically on the synaptosomal associated protein of 25 kDa (SNAP-25), BoNT serotypes B, D, F, and G cleave synaptobrevin, whereas BoNT serotype C cleaves both syntaxin and SNAP-25 (*11*). One of the unique features of BoNT endopeptidase acitivity is that while each of the BoNT serotypes have an identical $Zn^{2+}$ binding motif in their active sites, their substrates are either entirely different proteins or the cleavage site on the substrate is different for each serotype. Thus BoNTs display an extreme peptide bond cleavage selectivity within specific substrates (*1*).

Nicking of the single chain BoNT/E to the dichain form is associated with a 100-fold increase in toxicity (*12*, *13*). Spectroscopic analysis of BoNT/E has indicated structural changes associated with nicking (*12*). The molecular basis of nicking-mediated toxicity has not been clearly established, but an understanding of the molecular features responsible for increased toxicity could provide significant clues to the mechanism of action of the unique BoNT endopeptidases and the design of antidotes against botulism.

The crystal structures of botulinum neurotoxins reveal a heavy chain belt that occupies the substrate interaction site on the enzyme domain and the endopeptidase activities of BoNTs are

[†]This work was supported by DoD/Army Contract W911NF-06-1-0095 and by the National Institutes of Health through the New England Center of Excellence for Biodefense (Grant AI057159-01).

*Corresponding author. E-mail: bsingh@umassd.edu. Telephone: 508-999-8588. Fax: 508-999-8451.

[1]Abbreviations: BoNT, botulinum neurotoxin; LC, light chain; SNAP-25, synaptosomal associated protein of 25 kDa; VAMP, vesicle-associated membrane protein; SNARE, soluble NSF attachment protein receptor; NaPB, sodium phosphate buffer; CD, circular dichroism; SDS−PAGE, sodium dodecyl sulfate−polyacrylamide gel electrophoresis.

 Published on Web 02/23/2010 

observed only when their respective disulfide bonds are reduced. This issue is very important to understand the mechanistics of enzyme−substrate interaction when the toxin is intact with the heavy chain. The heavy chain belt is believed to displace for the substrate to effectively bind with the light chain endopeptidase (*14*), and reduction of the disulfide appears to facilitate this process. However, this hypothesis may be challenged in single chain BoNT, such as BoNT/E, providing a unique system not only to investigate this mechanism in its single and dichain forms but also to study the effect of the reduction of the disulfide bond on its structure and endopeptidase activity.

BoNT/E targets the same intracellular substrate, SNAP-25, as BoNT/A, but their cleavage sites are different (*11*). In addition, BoNT/A and BoNT/E have differential preference between the two isotypes of SNAP-25 (*15*) despite the absence of any difference in the cleavage site regions SNAP-25a or SNAP-25b for either BoNT/A or BoNT/E. Structural differences in the folding and dynamics are likely to resolve the basis of these differences. One of the differences between BoNT/A and BoNT/E is their respective dichain and single chain forms, which may play a role in their functional differences. Crystal structures of BoNT/A and BoNT/E, although showing dramatic differences in the topographical location of light and heavy chains (*14*, *16*), do not indicate likely differences at least between single and dichain forms (*16*). Thus a comparative structural analysis of BoNT/E, both in single and dichain forms, will provide a unique opportunity to compare with BoNT/A especially for its binding and recognition of SNAP-25.

In this report, we present the results of our investigation of the activation mechanism of BoNT/E, by nicking and subsequent reduction of the interchain disulfide bond. Reduction of the disulfide bond of even the unnicked single chain BoNT/E enhances its endopeptidase activity, but nicking itself, even without the reduction of the disulfide bond, enhances the endopeptidase activity to a large extent. It was also observed that at physiological temperatures the reduced form of nicked dichain BoNT/E adopts a dynamically flexible conformation and can cleave SNAP-25 maximally, suggesting a strong correlation between the flexible conformation of BoNT/E and its endopeptidase activity, a phenomenon similar to that observed in BoNT/A (*17*). Our observation of optimum activity of single chain BoNT/E endopeptidase at 50 °C has practical value of using it for assaying BoNT/E for its detection in biological fluids in which other interfering proteases will be denatured.

## EXPERIMENTAL PROCEDURES

*Purification and Nicking of Botulinum Neurotoxin Type E*. Single chain type E neurotoxin was isolated and purified from the cultures of *C. botulinum* type E strain Alaska according to the method described previously (*18*, *19*). The neurotoxin was nicked with trypsin (Sigma Chemical Co., St. Louis, MO) according to previously established procedures (*12*). Briefly, BoNT/E and trypsin were mixed in a ratio of 40:1 (w/w) and incubated at room temperature for 90 min. The reaction was stopped by incubating the mixture with soybean trypsin inhibitor linked to glass beads (Sigma Chemical Co., St. Louis, MO) for 30 min at room temperature. The nicked neurotoxin was recovered after centrifuging the glass beads. Both single chain and nicked neurotoxins were extensively dialyzed against 10 mM sodium phosphate buffer, pH 7.0, prior to being used for experiments. Concentration of the neurotoxin was determined using the extinction coefficient of 1.4 at 278 nm (*20*). Reduced BoNT/E was prepared by treating pure BoNT/E with 20 mM DTT for 30 min at 37 °C. The sample was then extensively dialyzed against 10 mM sodium phosphate buffer, pH 7.0, containing 1 mM DTT. For determining their purity and nicking, the proteins were analyzed by sodium dodecyl sulfate−polyacrylamide gel electrophoresis (SDS−PAGE) on a 8−20% gel using the PhastSystem (Pharmacia, NJ) electrophoresis system. The protein bands were visualized by Coomassie blue staining (Figure 1).

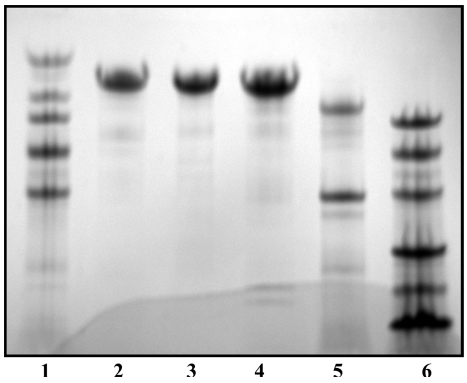


FIGURE 1: SDS−PAGE analysis of BoNT/E in its single and dichain forms under reducing and nonreducing conditions visualized by Coomassie blue staining: lane 1, high molecular mass protein marker (200.0, 116.3, 97.4, 66.2, and 45.0 kDa); lane 2, BoNT/E nonreduced single chain BoNT/E; lane 3, reduced single chain BoNT/E; lane 4, nonreduced dichain BoNT/E; lane 5, reduced dichain BoNT/E; lane 6, low molecular mass protein marker (97.4, 66.2, 45.0, 31.0, 21.5, and 14.4 kDa).

*Circular Dichroism Spectroscopy*. Circular dichroism (CD) spectra of single and dichain forms of BoNT/E under reducing and nonreducing buffer conditions were recorded using a Jasco J-715 spectrophotometer equipped with a Peltier temperature control system (Model PTC-348W). Far-UV CD spectra were recorded at wavelengths between 250 and 190 nm using a 0.1 cm path length cell containing 0.2−0.3 mg/mL protein dissolved in 10 mM sodium phosphate buffer, pH 7.0, at 20 °C. The scanning speed was set at 20 nm/min, and the response time was 8 s. Final spectra represented the average of at least five scans and were corrected for the buffer spectrum.

Thermal denaturation experiments were carried out by monitoring the ellipticity at 222 nm as a function of temperature. The temperature was raised from 20 to 90 °C with a heating rate of 2 °C/min. Thermodynamic data were analyzed as described previously (*21*).

*Surface Exposure of Tyrosine Residues Using UV Second Derivative Spectroscopy*. Absorption spectra of BoNT/E were recorded between 240 and 320 nm using a Jasco UV/vis spectrophotometer equipped with Peltier temperature control. The spectra were derivatized to the second order. The ratio of "a" (an arithmetic sum of the negative $d^2A/d\lambda^2$ at 285 nm and a positive $d^2A/d\lambda^2$ at 289 nm) and "b" (an arithmetic sum of the negative $d^2A/d\lambda^2$ at 291 nm and the positive $d^2A/d\lambda^2$ at 295 nm) was measured at different temperatures (where $A$ is the absorbance of BoNT/E). Exposure of tyrosine residues was analyzed according to the methods of Ragone et al. (*22*, *12*) using the equation:

$$A = [(\gamma_n - \gamma_a)/(\gamma_u - \gamma_a)] \times 100$$

where $\gamma_n$ and $\gamma_u$ are the derivative peak ratio (a/b) of BoNT/E at 25 and 37 °C, respectively. $\gamma_a$ is the derivative peak ratio of a mixture of free Tyr and Trp residues in the same molar ratio as

the neurotoxin. $\gamma_a$ for BoNT/E was calculated according to the equation $A_x + B/C_x + 1$, where $A$, $B$, and $C$ are constants (*22*) and $x$ is the Tyr/Trp molar ratio of BoNT/E.

*Fluorescence Spectroscopy*. Fluorescence measurements were carried out by measuring the fluorescence emission spectra of the BoNT/A and BoNT/E complex at 25 °C using an ISS K2 fluorometer (Champaign, IL). The excitation wavelength used was 295 nm, and both the excitation and emission slits were fixed at 8 nm. The absorbance at 295 mn was kept between 0.06 and 0.08 in order to minimize the inner filter effect. Emission spectra were recorded between 310 and 540 nm.

*Endopeptidase Activity Assay*. BoNT/E was assayed for endopeptidase activity using its intracellular target protein, SNAP-25, as substrate. Expression of recombinant $His_6$-tagged SNAP-25 was induced by addition of 1 mM IPTG at 37 °C for 3 h. The protein was isolated on a His-Bind column according to the previously established procedures (*23*). The effect of temperature on the endopeptidase activity of BoNT/E was examined by incubating 7.6 $\mu$M SNAP-25 with 200 nM reduced single chain BoNT/E, nonreduced dichain BoNT/E, and reduced dichain BoNT/E at the designated temperature for 30 min in an assay buffer (50 mM Tris-HCl, 10 mM sodium phosphate, 300 mM NaCl, 2 mM $MgCl_2$, 0.3 mM $CaCl_2$, and 0.1% $NaN_3$, pH 7.6). The cleavage reaction was terminated by addition of SDS−PAGE sample buffer, and the samples were heated in a boiling water bath for 5 min, followed by separation on a 10−20% SDS−PAGE gradient gel. The electrophoresis was carried out using a Mini Protean II system from Bio-Rad (Hercules, CA) at room temperature (25 °C) and at a constant voltage of 200 V. The bands on the gel were visualized by Coomassie blue staining. The amount of uncleaved SNAP-25 was scanned on a GEL LOGIC 100 Imager system, analyzed, and quantified using the Kodak Image analysis software (Eastman Kodak Co., Rochester, NY). The percentage of cleavage was estimated by comparing the density of the uncleaved SNAP-25 to that of the control SNAP-25.

## RESULTS

The structure−function relationships of single chain (unnicked) and dichain (nicked) forms of BoNT/E under reducing and nonreducing conditions in different stages of protein unfolding are examined using spectroscopic techniques to examine their impact on the functional state of the proteins. The major goal of this study was to determine structural differences between single and dichain BoNT/E and to correlate the structural attributes to the endopeptidase activity.

*Disulfide Bond Reduction Induces Structural Changes in Nicked BoNT/E*. The endopeptidase activity of all BoNT types has been demonstrated under conditions of either separated light chains or at least reduction of the disulfide bond between the light and heavy chains (*24*−*26*). Whereas reports have appeared which imply that disulfide reduction leads to separation of chains (*14*, *27*−*29*) making the active site accessible for substrate binding, structural analysis has not been carried out to examine changes in conformation that accompany disulfide bond reduction. A single chain BoNT/E provides an attractive model to test the hypothesis if chain separation is critical for the expression of endopeptidase activity, since chain separation is not possible even after the disulfide bond reduction. Circular dichroism, second derivative spectroscopy, and Trp fluorescence spectroscopy were used to examine the structural changes in BoNT/E (single and dichain forms) following reduction of the disulfide bond.

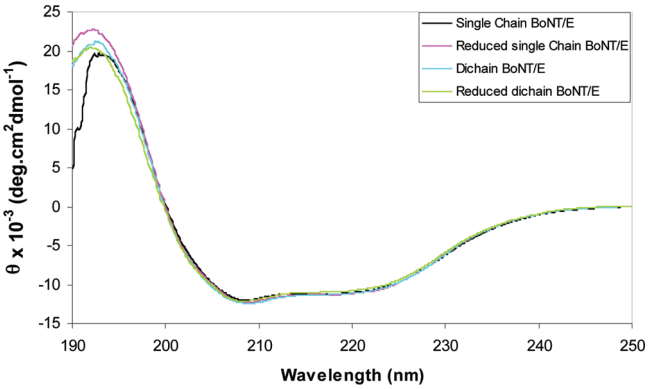


FIGURE 2: Far-UV CD spectrum of single chain BoNT/E, reduced single chain BoNT/E, dichain BoNT/E, and reduced dichain BoNT/E, dissolved in 10 mM sodium phosphate buffer, maintained at pH 7.0, and recorded at 20 °C.

*Secondary Structural Changes in BoNT/E Monitored by Circular Dichroism*. CD is sensitive to the protein conformation and hence is a convenient method for determining structural changes in proteins. The CD spectra of single chain BoNT/E, reduced single chain BoNT/E, dichain BoNT/E, and reduced dichain BoNT/E were found to be virtually indistinguishable from each other, all exhibiting negative double minima at 208 and 222 nm, characteristic of α-helix-rich proteins (*30*), as seen in Figure 2. The similar mean residue ellipticity values of all of the forms of BoNT/E indicated that they had similar secondary structural characteristics. This observation suggests that the neurotoxin retains its basic structural core upon nicking and is consistent with an earlier report wherein the secondary structure was not affected by nicking BoNT/E (*12*).

To evaluate the thermal stability of BoNT/E, we determined change in ellipticity at 222 nm ($\theta_{222}$) as a function of temperature. Thermal denaturation of proteins provides useful information concerning the nature and cooperativity of interactions stabilizing the structures. The temperature-dependent changes of the molar ellipticity were well described by a sigmoidal curve with an inflection point corresponding to the denaturing temperature. Although the thermal denaturation was irreversible, precluding true thermodynamic parameters, the transition curves based on the far-UV CD signals indicated apparent $T_m$ values of 53.5, 53.6, 52.9, and 54.1 °C for the unnicked BoNT/E, reduced form of unnicked BoNT/E, nicked BoNT/E, and the reduced form of nicked BoNT/E, respectively (Figure 3, Table 1). Although the $T_m$ values were found to be closely similar for all forms of BoNT/E, the temperature denaturation profile of reduced dichain BoNT/E was found to be different from the others. As seen in Figure 3, thermal unfolding of single chain BoNT/E, reduced single chain BoNT/E, and dichain BoNT/E occurs with a sharp transition of the native protein to the denatured form between 48 and 60 °C. However, the reduced form of dichain BoNT/E exhibits a relatively slow and smooth unfolding pattern from 38 to 60 °C. This relatively broad transition suggests a noncooperative unfolding which would be consistent of a nonrigid structure. This observation is supported by pseudothermodynamic parameters such as smaller $\Delta H$ and expected higher entropy (as reflected by smaller $\Delta S$ in Table 1) of reduced dichain BoNT/E at 20 °C. It is notable that nicking itself did not introduce any significant instability, as demonstrated by similar $\Delta H$ and $\Delta S$ values for single and dichain BoNT/E under nonreduced conditions (Table 1).

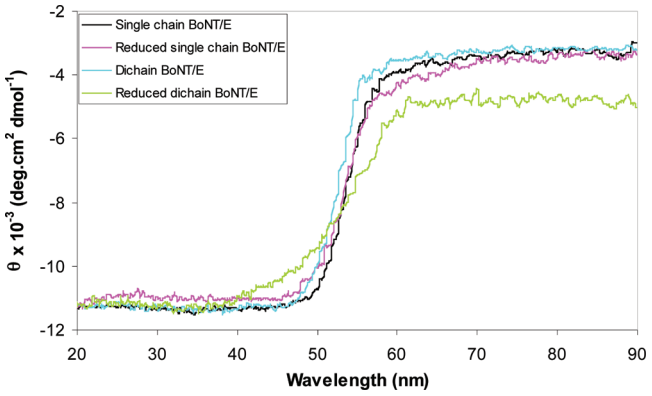


FIGURE 3: Thermal denaturation profile of single chain BoNT/E, reduced single chain BoNT/E, dichain BoNT/E, and reduced dichain BoNT/E, dissolved in 10 mM sodium phosphate buffer, maintained at pH 7.0, and monitored by recording the CD signal at 222 nm. Sample was heated at a rate of 2 °C/min.

Table 1: Thermodynamic Parameters for Temperature-Induced Denaturation of BoNT/E Based on the CD Signal at 222 nm

| protein | $\Delta H$ (kJ/mol) | $\Delta S$ (J/(K·mol)) | $\Delta G$ (kJ/mol) | $T_m$ (°C) |
|---|---|---|---|---|
| single chain BoNT/E | 233.7 ± 3.8 | 709.4 ± 11.3 | 22.5 ± 0.3 | 53.5 ± 0.3 |
| reduced single chain BoNT/E | 226.4 ± 0.8 | 673.6 ± 15.3 | 21.6 ± 0.2 | 53.6 ± 0.2 |
| dichain BoNT/E | 230.6 ± 3.4 | 698.6 ± 13.5 | 22.1 ± 0.4 | 52.9 ± 0.4 |
| reduced dichain BoNT/E | 171.6 ± 4.7 | 519.5 ± 12.5 | 16.8 ± 0.3 | 54.1 ± 0.2 |

However, the enthalpic requirement for the denaturation of reduced dichain BoNT/E is 27% less than that of unreduced BoNT/E. In addition, reduced BoNT/E shows over 27% entropic instability compared to the nonreduced BoNT/E. The free energy change ($\Delta G$) for the unfolding of the nonreduced dichain BoNT/E was 26% higher compared to its reduced form (Table 1), suggesting that the unfolding transition for the reduced form of dichain BoNT/E is more spontaneous than for the nonreduced form. These results suggest a higher degree of flexibility in the polypeptide folding of the reduced form of dichain BoNT/E. Hence the temperature-dependent unfolding results suggest that disulfide reduction in the nicked form of BoNT/E introduces specific structural changes in the protein.

*Tertiary Structural Changes in BoNT/E Monitored by UV/Vis Absorbance and Fluorescence Spectroscopy*. Tertiary structural changes were estimated by monitoring surface/solvent accessibility of aromatic amino acid residues and thermal unfolding of BoNT/E.

Comparative polypeptide folding of single chain BoNT/E and dichain BoNT/E in both reduced and nonreduced forms was analyzed in terms of topography of Trp residues using fluorescence emission spectroscopy upon excitation of the samples at 295 nm at 25 °C. All of these forms of BoNT/E exhibited identical scans with emission maximum at 331 nm indicating identical surface accessibility of Trp residues in these forms (data not shown).

UV second derivative spectroscopy is a very useful probe for monitoring conformational changes occurring in proteins that affect the environment of Tyr residues (*12*, *19*).

The UV absorption spectra of single chain BoNT/E, reduced single chain BoNT/E, dichain BoNT/E, and reduced dichain BoNT/E were recorded between 240 and 320 nm and were derivatized to the second order. Polypeptide folding of BoNT/E was further analyzed by folding and unfolding patterns as a function of temperature. Unfolding of the neurotoxin was followed by monitoring the exposure of tyrosine residues which was in turn monitored by examining changes in the a/b ratio as a function of temperature. Changes in a/b ratio between native and unfolded forms of proteins is related to the changes in microenvironments of tyrosine residues which become more polar following protein denaturation.

It was observed that with increasing temperatures the a/b ratios were altered significantly. In the case of single chain BoNT/E, the a/b ratio was found to decrease with increasing temperatures. The a/b ratios at 25 and 45 °C were found to be 2.3 ±0.1 and 1.5 ± 0.1, respectively, reflecting a decrease of 36% in the a/b ratio (Figure 4B). Beyond 45 °C, it was difficult to accurately measure the peak ratios due to noise in the spectrum which may indicate the beginning of aggregation of the protein upon heating. A marked decrease in the a/b ratio upon heating indicates less exposure of tyrosine residues (*20*). A lower exposure may indicate either a refolding in the proteins resulting from exposure to a nonpolar environment or a tighter construction of the protein near the tyrosine residues. We prefer the first explanation, as it is difficult to conceive a tighter construction of the protein upon heating, unless we assume precipitation, which was not apparent in the samples. In any case, our observation suggests that significant changes in the polypeptide folding of single chain BoNT/E occur upon heating.

The reduced form of the single chain BoNT/E also displayed a similar pattern. Upon heating, there was a constant decrease in the a/b ratio. The second derivative spectrum could be accurately recorded up to 45 °C. The a/b ratios at 25 and 45 °C were 2.2 ± 0.1 and 1.7 ± 0.0, respectively, reflecting a 23% decrease (Figure 4B).

After nicking, the neurotoxin behaved differently. It was observed that with increase in temperature to 35 °C the a/b ratio decreased. However, when the protein was further heated to 37 °C, there was a slight increase in a/b ratio, indicating exposure of tyrosine residues at this temperature. Upon further heating, the a/b ratio continued to decrease up to 50 °C beyond which the ratios could not be accurately measured (Figure 4B).

Interestingly, the reduced form of the nicked BoNT/E exhibited a dramatically different unfolding pattern. It was observed that with increasing temperatures the a/b ratio continually increased up to 37 °C in contrast to the behavior of the nonreduced form of the nicked neurotoxin. At 37 °C, maximum exposure of Tyr residues was observed, suggesting that the Tyr residues are more mobile at this temperature. The a/b ratios at 25 and 37 °C were 2.0 ± 0.0 and 2.5 ± 0.1, respectively (Figure 4). Thus an increase of 20% in the a/b ratio was observed at 37 °C from that at 25 °C. The calculated fraction of tyrosine residues exposed to solvent at this temperature was 84.8%. Thus of the 67 Tyr residues in BoNT/E neurotoxin, 56 are exposed at 37 °C in the reduced form of the nicked neurotoxin. Upon further heating, the a/b ratio decreased up to 45 °C. At 50 °C the a/b ratio remained virtually the same as that at 45 °C (Figure 4B). Beyond this temperature (50 °C) the derivative peak positions could not be accurately measured.

A 1.2-fold higher Tyr exposure in reduced dichain BoNT/E at 37 °C compared to the nonreduced form suggests that the peptide segments containing exposed Tyr residues are more accessible to the surface in the reduced nicked neurotoxin than in the nonreduced form. A significant change in the polypeptide folding is likely to affect the degree of tyrosine residues exposed to the

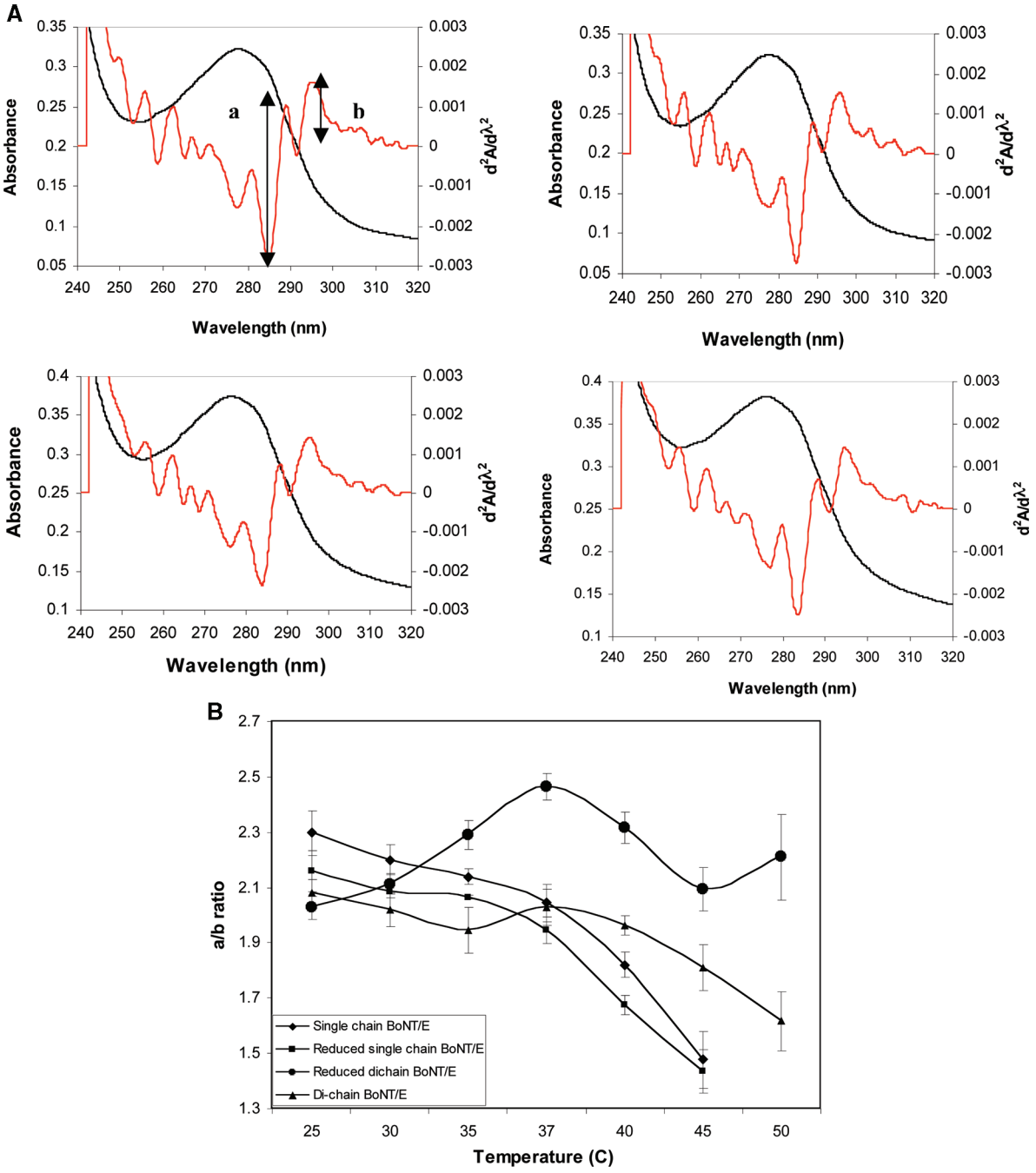


FIGURE 4: (A) Absorption and second derivative spectra of reduced dichain BoNT/E dissolved in 10 mM sodium phosphate buffer, pH 7.0, at 25 °C (top left), 37 °C (top right), 45 °C (bottom left), and 50 °C (bottom right). "a" represents the arithmetic sum of the negative $d^2A/d\lambda^2$ at 285 nm and a positive $d^2A/d\lambda^2$ at 289 nm, and "b" represents the arithmetic sum of the negative $d^2A/d\lambda^2$ at 291 nm and the positive $d^2A/d\lambda^2$ at 295 nm. (B) Effect of increasing temperature on the second derivative ratio (a/b) of single chain BoNT/E, reduced single chain BoNT/E, dichain BoNT/E, and reduced dichain BoNT/E dissolved in 10 mM NaPB, pH 7.0.

protein surface. Since Tyr residues are hydrophobic in nature, their greater accessibility may reflect more flexibility in the polypeptide folding of the reduced dichain BoNT/E.

*Enhancement of Endopeptidase Activity of BoNT/E upon Nicking and Reduction of Disulfide Bond.* Endopeptidase activities of reduced single chain BoNT/E, dichain BoNT/E, and reduced dichain BoNT/E were analyzed by their ability to proteolytically cleave recombinant SNAP-25 protein as a function of temperature. Under nonreducing conditions, single chain BoNT/E has been shown to exhibit practically no endopeptidase activity (*31*). Hence only the reduced form of single chain BoNT/E was assayed for enzymatic activity.

It was observed that the reduced form of single chain BoNT/E at 200 nM concentration cleaved about 22% of SNAP-25 at 37 °C. It displayed maximum activity at 45 °C, leading to an average cleavage of 78% (Figure 5). BoNT/E in its dichain (nicked) form exhibits an increase in functional stability of the neurotoxin against temperature as it was able to optimally cleave 77% of SNAP-25 at 50 °C (Figure 5).

Reduction of the disulfide bond in dichain BoNT/E introduced major changes in its enzymatic activity at different temperatures. Upon reduction of the disulfide bond, the endopeptidase activity of the nicked BoNT/E reached a maximum at the physiological temperature of 37 °C as revealed by the 77%

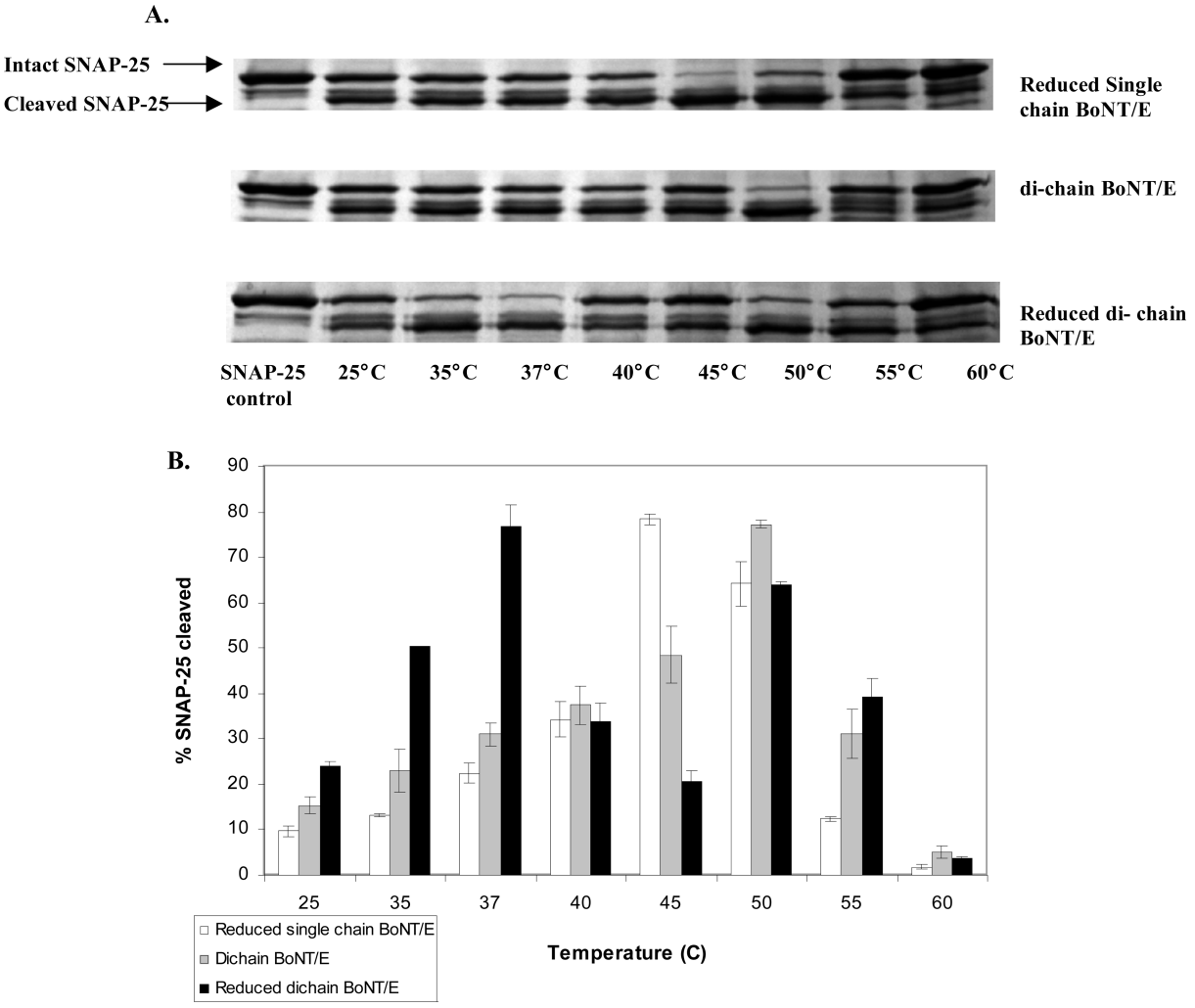


FIGURE 5: (A) SDS−PAGE analysis of endopeptidase activity of reduced single chain BoNT/E, dichain BoNT/E, and reduced dichain BoNT/E at different temperatures using SNAP-25 as its substrate. 7.6 $\mu$M SNAP-25 was incubated with 200 nM reduced BoNT/E at varying temperatures for 30 min. (B) Comparative endopeptidase activity analysis of reduced single chain BoNT/E, dichain BoNT/E, and reduced dichain BoNT/E as a function of temperature. Cleavage percentage of SNAP-25 by the neurotoxins was monitored at varying temperatures. The error bars represent the standard deviation of three independent experiments.

cleavage of SNAP-25 (Figure 5), which is a 2.5-fold enhancement from the endopeptidase activity of the nicked form of BoNT/E under nonreducing conditions at 37 °C. As the temperature was further increased to 45 °C, the endopeptidase activity dramatically decreased, exhibiting only a 21% cleavage of SNAP-25 at 45 °C. Interestingly, at 50 °C, its enzymatic activity again increased, and it was able to cleave 64% SNAP-25 at this temperature (Figure 5). Beyond this temperature, the endopeptidase activity reduced significantly, and by 60 °C, it only displayed minimal residual activity (4%) (Figure 5). These observations suggest that the endopeptidase activity of BoNT/E is greatly augmented upon nicking and reduction of the disulfide bond.

## DISCUSSION

The endopeptidase activity of BoNT provides many unique characteristics to attract attention not only for its physiological role in causing the botulism disease but also for understanding the mechanistics of enzyme selectivity and specificity. Generally, each of the seven serotypes of BoNT targets one of the three components of the SNARE complex involved in the exocytosis process selectively cleaving exclusive sites (*1*, *10*, *32*). The fact that the endopeptidases of all the serotypes target a process (exocytosis) rather than a particular protein in the overall process is intriguing. An effort has been made to identify a SNARE motif (*33*) to explain common features of enzyme substrate being recognized by all BoNT serotypes. However, the recent cocrystal structure of BoNT/A and its substrate, SNAP-25 (*34*), revealed exosites in addition to the active site on BoNT/A L chain, but those exosites were not shown to interact with the SNARE motifs of the SNAP-25. Therefore, the structure of biologically active BoNT capable of productive binding with its substrate is still not clear.

The endopeptidase activity of BoNTs is expressed in the holotoxin (consisting of L and H chains) only when the disulfide bond linking the two chains is reduced (*24*, *25*, *21*). This phenomenon has been generally explained by the suggestion that the reduction of the disulfide bond relaxes the belt surrounding the light chain, resulting in the exposure of the endopeptidase active site to the substrate (*14*). However, the crystal structure of BoNT/B under reducing and nonreducing conditions showed no difference in the polypeptide folding (*1*), suggesting a mechanism that might be related to the dynamic rather than the static structure of the protein. Furthermore, chain separation is suggested upon disulfide bond reduction, a process unlikely to happen given noncovalent interactions involved between the

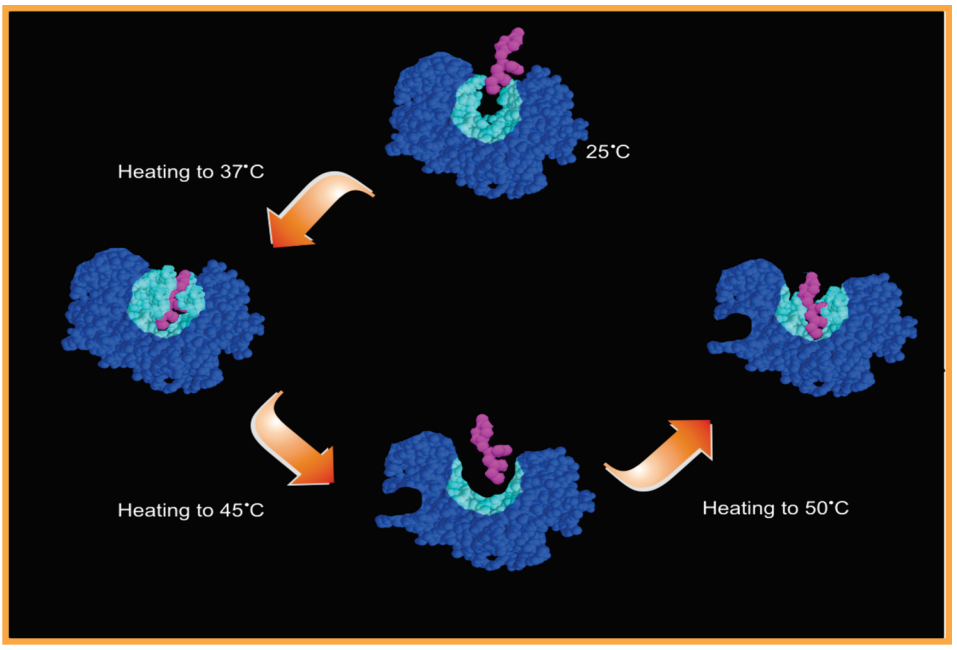


FIGURE 6: Schematic cartoon representation of the activation of the endopeptidase activity of BoNT/E upon nicking and reduction of disulfide bond facilitating binding and subsequent cleavage of its substrate, SNAP-25, at varying temperatures. The substrate, SNAP-25, is represented by the magenta molecule. The enzyme (reduced form of nicked BoNT/E) is represented by blue and cyan colors. The cyan-colored structure is used to more sharply define the active site. At 25 °C, the enzyme does not interact efficiently with the substrate and exhibits only 25% of endopeptidase activity. At 37 °C, the enzyme adapts a higher degree of flexibility in its polypeptide folding facilitating maximum interaction with SNAP-25. The polypeptide chains being flexible fit around the substrate. This subsequently leads to optimal cleavage of SNAP-25. Upon further heating to 45 °C, the enzyme is distorted to the degree that it is not capable of binding efficiently to the substrate, and it retains 25% of its optimal activity. At 50 °C, however, the enzyme again experiences some flexibility, and its interaction with SNAP-25 is suboptimal, leading to around 80% of its optimal endopeptidase activity.

two chains. This issue is very important to understand the mechanistics of enzyme−substrate interaction when the toxin is intact with the heavy chain, particularly in a single chain form. Recently, an idea has been advanced based on studies with crystal structures and recombinant proteins corresponding to the BoNT/A light chain (*35*−*37*), which proposes that for binding of the substrate the heavy chain belt needs to be displaced from its binding track on the light chain so that the same track is utilized by the substrate to bind to the light chain. It is possible to assume that disulfide reduction in the dichain BoNT might allow displacement of the belt; disulfide reduction of the single chain BoNT is unlikely to allow for such a relaxation as the domains of the two chains still remain covalently linked as a single polypeptide.

BoNT/E provides a unique system not only to investigate this mechanism of action in the single and dichain forms but also to study the effect of reduction of the disulfide bond on its structure and endopeptidase activity, as some of these questions can be addressed by examining the structure and endopeptidase activity of BoNT/E in its single chain form and comparing it with the dichain form with and without the reduction of the disulfide bond.

Transformation of single chain BoNT/E into the dichain form is well-known to enhance its toxicity (*12*). However, the molecular basis of this activation is not clearly understood. While the far-UV CD spectra and the temperature denaturation curves show no apparent distinction in single and dichain BoNT/E (Figures 2 and 3), the temperature-dependent changes in Tyr exposure suggest that significant differences are introduced in the polypeptide folding of single chain BoNT/E upon its nicking into the dichain (Figure 4). Interestingly, reduction of the disulfide bond in the single chain BoNT/E showed minimal variation from the nonreduced form, but reduction of the dichain BoNT/E showed a dramatically different temperature-induced profile of changes in Tyr exposure as shown by a substantial peak in the a/b ratio at 37 °C.

The most dramatic observations in this study are the optimum temperature of endopeptidase activity in the reduced single and dichain BoNT/E and the unreduced dichain BoNT/E (Figure 5). The three samples showed optimum endopeptidase activity at 45 (single chain BoNT/E) or 50 °C (dichain BoNT/E), and reduced dichain BoNT/E showed two temperature optima (37 and 50 °C). While maximum activity at 37 °C is understandable and has been observed for BoNT/A (*17*, *21*), the maximum at 45 or 50 °C is entirely unexpected given the spectroscopic data showing significant loss of the secondary structure (Figure 3) which is accompanied by substantial change in the tertiary structure (Figure 4). The increased dynamic flexibility at this stage could play an important role in the favorable interactions of SNAP-25 with BoNT/E at this temperature.

The reduced form of dichain BoNT/E displayed maximum exposure of Tyr residues at the physiological temperature of 37 °C and optimum endopeptidase activity at this temperature. Changes in Tyr exposure as a function of temperature suggested increased intramolecular mobility and the presence of a loose hydrophobic core in the reduced form of the nicked BoNT/E at 37 °C relative to that at 25 °C. This conformation of BoNT/E favors maximum specific binding with SNAP-25 leading to the optimal cleavage of the latter, an observation that is consistent with the temperature profile of BoNT/A endopeptidase activity (*17*). It is likely that the relatively tighter tertiary structure at 37 °C in the single chain form may not have adequate groups available for its interaction with the substrate protein. Figure 6 is a schematic cartoon representation of the activation of

endopeptidase activity of BoNT/E upon nicking and reduction of the disulfide bond that may facilitate the binding and subsequent cleavage of SNAP-25 at varying temperatures. The nonreduced form of dichain BoNT/E displayed maximum enzymatic activity at 50 °C, further favoring the strong correlation between protein flexibility and enzyme functionality. The reduced form of dichain BoNT/E was also found to exhibit significantly higher activity at 50 °C after reduction in the enzyme activity at 40 and 45 °C (Figure 5). At this temperature the enzyme activity of reduced single and dichain BoNT/A, while significantly different from the nonreduced dichain BoNT/E, is identical, suggesting the strong influence of the disulfide bond reduction on the folding of the protein. Since the denaturation curves monitored in terms of both far-UV CD (secondary structure) and second derivative UV spectroscopy (Tyr exposure) look quite different for these two samples (reduced form of single and dichain BoNT/E), the function would have to be related to either the remaining secondary structure features of the two proteins or a degree of dynamic interactions allowed equally in reduced single and dichain BoNT/E at 50 °C.

Unreduced dichain BoNT/E shows optimum enzyme activity at 50 °C than the reduced dichain BoNT/E (Figure 5), perhaps owing to the restricted flexibility of critical domains due to the disulfide bond. Reappearance of enzyme activity in reduced dichain BoNT/E at 50 °C could be due to either its less than optimum interaction with SNAP-25 or decreased catalytic efficiency of the enzyme, leading to around 80% of its optimal endopeptidase activity. The point will be clarified with further research to obtain enzyme kinetic parameters and binding constants. This phenomenon of double optimal activity in BoNT/E is unique and very different from the behavior of BoNT/A (data not shown).

An application of BoNT/E endopeptidase activity may include detection of enzymatically active BoNT/E in environmental samples and biological fluids. Detection of BoNT and confirming its biological activity are very important for taking preventive and corrective measures (*38*, *39*). A major problem in determining the endopeptidase activity in biological fluids is the interference from other proteases present. However, such proteases are denatured at 50 °C, thus allowing BoNT/E endopeptidase activity to be measured exclusively.

Protein function is largely dependent on the maintenance of an appropriate balance between molecular stability and structural flexibility (*40*). The ability to easily move between closely related conformations forms the basis of enzyme functionality. Since conformational motions of enzymes that are functionally important require thermal energy from the surrounding medium, temperature plays an important role in enzyme flexibility (*40*). The pseudothermodynamic parameters derived from the thermal denaturation curves indicate that the reduced form of nicked BoNT/E adapts a higher degree of flexibility in its polypeptide folding (Table 1). The reduction of the disulfide bond in general is known to lead to protein instability (*41*) and, in this case, is sufficient to introduce changes in BoNT/E to enhance its endopeptidase activity even at 37 °C.

The solution structural information of BoNTs has indicated a more flexible structure upon reduction of the disulfide bond (*21*, *42*). It has recently been shown that the activation mechanism of BoNT/A by reduction of the interchain disulfide bond involves a molten globule state under physiological temperature conditions (*17*). The nonreduced form of BoNT/A, on the other hand, does not exist in such a conformation. Examination of the biological activity suggests that the molten globule state of BoNT/A under reducing conditions is the enzymatically active structure (*17*). Hence the flexible conformation of reduced BoNT/A at physiological temperature is highly related to its endopeptidase activity and therefore plays a critical role in the intracellular intoxification process. BoNT/E in its reduced dichain form adapts a higher degree of flexibility in its polypeptide folding at 37 °C and can optimally cleave SNAP-25 at this temperature. Thus like BoNT/A, there may exist a strong correlation between this flexible conformation of BoNT/E at the physiological temperature and its endopeptidase activity.

The crystal structures of BoNT/A and BoNT/B holotoxin and more recently of BoNT/E have been resolved (*14*, *43*, *16*). The X-ray crystallographic structure of BoNT/A provides a clue to the possible role of disulfide reduction in the activation of BoNT/A endopeptidase activity. The active site in BoNT/A is buried 20−24 Å deep in the protein matrix and is partially shielded by a belt from the N-terminal domain of the heavy chain involved in the disulfide bond formation (*14*). The reduction of the disulfide bond presumably allows accessibility of the active site to the substrate. In BoNT/B, however, the active site is buried only 16 Å deep, and the belt from the N-terminal region of the heavy chain does not occlude the active site of the protein (*43*). Nevertheless, BoNT/B requires reduction of the disulfide bond between the light and heavy chains for activation of its endopeptidase activity (*44*). The recent X-ray crystal structure of BoNT/E holotoxin indicates a unique domain organization wherein the catalytic and binding domain are on the same side of the translocation domain much unlike that of BoNTs A and B (*16*). The double optima feature of the endopeptidase activity of BoNT/E is also a significant uniqueness of BoNT/E. Could these structural and functional features be correlated? There is no obvious relationship. Furthermore, it notable that crystallization of BoNT/E was reportedly difficult apparently due to the flexibility of the structure (*16*). Such a flexibility is not predictable from the denaturation curves of BoNT/E which show sharp denaturation transition, at least under single chain conditions (Figure 3). A notable observation made in the crystal structure of single chain BoNT/E that the unique organization of catalytic and binding domains vis á vis BoNT/A is not due to the nicking may have to be considered tentative as we have observed substantial structural differences in the denaturation of single and dichain BoNT/E, at both the secondary and tertiary structure levels (Figures 3 and 4). The dichain BoNT/E showed denaturation in two phases at the tertiary structural level (in terms of Tyr exposure), which may be related to a multistate denaturation process, generally reflective of independent unfolding of domains or subunits. A compact structure shown in the crystal structure may be different at least in the reduced form of the dichain BoNT/E in solution, based on its broad unfolding process and double enzyme activity maxima, both reflective of flexible structures even at 50 °C.

Although crystallographic data provide useful information on the general folding patterns of BoNTs, there is a lack of consistent structural information of the biologically active enzyme. Structural characteristics in solution reveal a major role of the dynamic structure in the functioning of the molecule which is important for the design of effective inhibitors. It has been already observed that inhibitors identified in in vitro experiments seem to not work under in vivo conditions and vice versa (*45*), or the endopeptidase active site shows substantial flexibility (*46*), suggesting that structural dynamics may play a major role in the

interaction of BoNT endopeptidase to the inhibitors. An understanding of molecular mechanism of action of botulinum neurotoxin may suggest a variety of ways to inhibit their action and rescue poisoned nerve cells. Our observations with single and dichain BoNT/E, that rather than a static structure it may be the dynamics of the protein folding that plays a significant role in enzyme−substrate interaction, may open new avenues to counter and utilize these toxic proteins.

In summary, we have characterized the structure of BoNT/E in single and dichain forms in terms of surface accessibility of Tyr and Trp residues and correlated their structural traits with the expression of enzymatic activity. Surface accessibility of Tyr residues appears to play an important role in the active endopeptidase structure of BoNT/E. Reduction of the disulfide bond induces exposure of the hydrophobic segments introducing flexibility in the polypeptide folding in the nicked form of BoNT/E. Such reduction-induced increase in the flexibility of the polypeptide folding provides a rationale for the mechanism of BoNT/E endopeptidase against its intracellular substrate, SNAP-25, even at the unusually high temperature of 50 °C.

## REFERENCES


1. Singh, B. R. (2006) Botulinum neurotoxin structure, engineering, and novel cellular tafficking and targeting. *Neurotoxicity Res. 9*, 73–92.
2. Caya, J. G., Agni, R., and Miller, J. E. (2004) *Clostridium botulinum* and the clinical laboratorian. *Arch. Pathol. Lab. Med. 128*, 653–662.
3. Cai, S., and Singh, B. R. (2007) Botulism diagnostics: from clinical symptoms to *in vitro* assays. *Crit. Rev. Microbiol. 33*, 109–125.
4. Klein, A. W. (2004) Therapeutic potential of botulinum toxin. *Dermatol. Surg. 30*, 452–455.
5. Bigalke, H., and Rummel, A. (2005) Medical aspects of toxin weapons. *Toxicology 214*, 210–220.
6. Dastoor, S. F., Misch, C. E., and Wang, H. L. (2007) Botulinum toxin (Botox) to enhance facial macroesthetics: a literature review. *J. Oral Implantol. 33*, 164–171.
7. Aoki, K. R., and Guyer, B. (2001) Botulinum toxin type A and other botulinum toxin serotypes: a comparative review of biochemical and pharmacological actions. *Eur. J. Neurol. 8*, 21–29.
8. Singh, B. R. (2002) in Scientific and Therapeutic Aspects of Botulinum Toxin (Brin, M. F., Jankovic, J., and Hallet, M., Eds.) pp 75−88, Lipincott Williams and Wilkins, Philadelphia, PA.
9. Menestrina, G., Schiavo, G., and Montecucco, M. (1994) Molecular mechanisms of action of bacterial protein toxins. *Mol. Aspects Med. 15*, 79–193.
10. Poulain, B., Popoff, M., and Molgó, J. (2008) How do the botulinum neurotoxins block neurotransmitter release: from botulism to the molecular mechanism of action. *Botulinum J. 1*, 14–87.
11. Schiavo, G., Matteoli, M., and Montecucco, C. (2000) Neurotoxins affecting neuroexocytosis. *Physiol Rev. 80*, 717–755.
12. Singh, B. R., and DasGupta, B. R. (1990) Conformational changes associated with the nicking and activation of botulinum neurotoxin type E. *Biophys. Chem. 38*, 123–130.
13. DasGupta, B. R., and Sugiyama, S. (1977) in Perspectives in Toxinology (Bernheimer, A. W., Ed.) pp 87−119, John Wiley and Sons, New York.
14. Lacy, D. B., Tepp, W., Cohen, A. C., DasGupta, B. R., and Stevens, R. C. (1998) Crystal structure of botulinum neurotoxin type A and implications for toxicity. *Nat. Struct. Biol. 5*, 898–902.
15. Puffer, E. B., Lomneth, R. B., Sarkar, H. K., and Singh, B. R. (2001) Differential roles of developmentally distinct SNAP-25 isoforms in the neurotransmitter release process. *Biochemistry 40*, 9374–9378.
16. Kumaran, D., Eswaramoorthy, S., Furey, W., Navaza, J., Sax, M., and Swaminathan, S. (2009) Domain organization in *Clostridium botulinum* neurotoxin type E is unique: its implication in faster translocation. *J. Mol. Biol. 386*, 233–245.
17. Cai, S., and Singh, B. R. (2001) Role of the disulfide cleavage induced molten globule state of type A botulinum neurotoxin in its endopeptidase activity. *Biochemistry 40*, 15327–15333.
18. Gimenez, J. A., and Sugiyama, H. (1987) Simplified purification method for clostridium botulinum type E toxin. *Appl. Environ. Microbiol. 53*, 2827–2830.
19. Singh, B. R., Foley, J., and Lafontaine, C. (1995) Physicochemical and immunological characterization of type E botulinum neurotoxin binding protein purified from *Clostridium botulinum*. *J. Protein Chem. 14*, 7–18.
20. Singh, B. R., and DasGupta, B. R. (1989) Structure of heavy and light chain subunits of type A botulinum neurotoxin analyzed by circular dichroism and fluorescence measurements. *Mol. Cell. Biochem. 86*, 87–95.
21. Cai, S., Sarkar, H. K., and Singh, B. R. (1999) Enhancement of the endopeptidase activity of botulinum neurotoxin by its associated proteins and dithiothreitol. *Biochemistry 38*, 6903–6910.
22. Ragone, R., Colonna, G., Balestrieri, C., Servillo, L., and Irace, G. (1984) Determination of tyrosine exposure in proteins by second-derivative spectroscopy. *Biochemistry 23*, 1871–1875.
23. Li, L., and Singh, B. R. (1999) High-level expression, purification, and characterization of recombinant type A botulinum neurotoxin light chain. *Protein Expression Purif. 17*, 339–344.
24. Schiavo, G., Rossetto, O., Santucci, A., DasGupta, B. R., and Montecucco, C. (1992) Botulinum neurotoxins are zinc proteins. *J. Biol. Chem. 267*, 23479–23483.
25. Blasi, J., Chapman, E. R., Link, E., Binz, T., Yamasaki, S., De camilli, P., Südhof, T. C., Niemann, H., and Jahn, R. (1993) Botulinum neurotoxin A selectively cleaves the synaptic protein SNAP-25. *Nature 365*, 160–163.
26. Humeau, Y., Doussau, F., Grant, N. J., and Poulain, B. (2000) How botulinum and tetanus neurotoxins block neurotransmitter release. *Biochimie 82*, 427–446.
27. Simpson, L. L., Maksymowych, A. B., Park, J. B., and Bora, R. S. (2004) The role of the interchain disulfide bond in governing the pharmacological actions of botulinum toxin. *J. Pharmacol. Exp. Ther. 308*, 857–864.
28. Fischer, A., and Montal, M. (2007) Crucial role of the disulfide bridge between botulinum neurotoxin light and heavy chains in protease translocation across membranes. *J. Biol. Chem. 282*, 29604–29611.
29. Breidenbach, M. A., and Brunger, A. T. (2005) New insights into clostridial neurotoxin-SNARE interactions. *Trends Mol. Med. 11*, 377–381.
30. Woody, R. W. (1995) Circular dichroism. *Methods Enzymol. 246*, 34–71.
31. Sharma, S., and Singh, B. R. (2004) Enhancement of the endopeptidase activity of purified neurotoxins A and E by an isolated component of the native neurotoxin associated proteins. *Biochemistry 43*, 4791–4798.
32. Kukreja, R., and Singh, B. R. (2009) in Microbial Toxins: Current Research and Future Trends (Proft, T., Ed.) pp 15−40, Caister Academic Press, New York.
33. Montecucco, C., and Schiavo, G. (1995) Structure and function of tetanus and botulinum neurotoxins. *Q. Rev. Biophys. 28*, 423–472.
34. Breidenbach, M. A., and Brunger, A. T. (2004) Substrate recognition strategy for botulinum neurotoxin serotype A. *Nature 432*, 925–929.
35. Brunger, A. T., Breidenbach, M. A., Jin, R., Fisher, A., Santos, J. S., and Montal, M. (2007) Botulinum neurotoxin heavy chain belt as an intramolecular chaperone for the light chain. *PLoS Pathog. 3*, 1191–1194.
36. Chen, S., Hall, C., and Barbieri, J. T. (2008) Substrate recognition of VAMP-2 by botulinum neurotoxin B and tetanus neurotoxin. *J. Biol. Chem. 283*, 21153–21159.
37. Kumaran, D., Rawat, R., Ahmed, S. A., and Swaminathan, S. (2008) Substrate binding mode and its implication on drug design for botulinum neurotoxin A. *PLoS Pathog. 4*, e1000165.
38. Cai, S., Singh, B. R., and Sharma, S. (2007) Botulism diagnostics: from clinical symptoms to in vitro assays. *Crit. Rev. Microbiol. 33*, 109–125.
39. Sharma, S., Cai, S., and Singh, B. R. (2008) Here a method, there a method, everywhere many methods. What should a laboratory do to validate an assay for the detection of botulinum neurotoxins? *Botulinum J. 1*, 183–198.
40. Fields, P. A. (2001) Protein function at thermal extremes: balancing stability and flexibility. *Comp. Biochem. Physiol. 129*, 417–431.
41. Betz, S. F. (1993) Disulfide bonds and the stability of globular proteins. *Protein Sci. 10*, 1551–1558.
42. Cai, S., and Singh, B. R. (2001) A correlation between differential structural features and the degree of endopeptidase activity of type A botulinum neurotoxin in aqueous solution. *Biochemistry 40*, 4693–4702.
43. Swaminathan, S., and Eswaramoorthy, S. (2000) Structural analysis of the catalytic and binding sites of *Clostridium botulinum* neurotoxin B. *Nat. Struct. Biol. 7*, 693–699.
44. Schiavo, G., Benfenati, F., Poulain, B., Rossetto, O., Polverino de Laureto, P., DasGupta, B. R., and Montecucco, C. (1992)

Tetanus and botulinum-B neurotoxins block neurotransmitter release by a proteolytic cleavage of synaptobrevin. *Nature 359*, 832–835.
45. Eubanks, L. M., Hixon, M. S., Jin, W., Hong, S., Clancy, C. M., Tepp, W. H., Baldwin, M. R., Malizio, C. J., Goodnough, M. C., Barbieri, J. T., Johnson, E. A., Boger, D. L., Dickerson, T. J., and Janda, K. D. (2007) An in vitro and in vivo disconnect uncovered through high-throughput identification of botulinum neurotoxin A antagonists. *Proc. Natl. Acad. Sci. U.S.A. 104*, 2602–2607.
46. Silvaggi, N. R., Boldt, G. E., Hixon, M. S., Kennedy, J. P., Tzipori, S., Janda, K. D., and Allen, K. N. (2007) Structures of *Clostridium botulinum* neurotoxin serotype A light chain complexed with small-molecule inhibitors highlight active-site flexibility. *Chem. Biol. 14*, 533–542.